U.S. DEPARTMENT OF COMMERCE
Patent and Trademark Office

DOCUMENT RETRIEVAL REQUEST FORM

Requester's Name: Fred Ferris		Case Serial Number: None	Art Unit/Org.: 2123
Phone: 305-9670	Fax:	Building: PK2	Room Number: 5D53
Date of Request: 10/01/03		Date Needed By:	

Paste or add text of citation or bibliography: **Paste Citation** Only one request per form. Original copy only. ☐

Author/Editor:	
Book Title:	
Article Title:	
Volume Number:	Report Number: Pages:
ISBN Number:	Series Number: Year of Publication:
Publisher:	
31 Remarks:	

Library Action	PTO		LC		NAL		NIH		NLM		NIST		Other	
	1st	2nd	1st	2nd	1st	2nd	1st	2nd	1st	2nd	1st	2nd	1st	2nd
Local Attempts	X													
Date	10/2													
Initials	nd													
Results	COMPLETED													
Examiner Called														
Page Count														
Money Spent														

	Source	Date
Remarks/Comments 1st and 2nd denotes time taken to a library O/N – Under NLM means Overnight	**Ordered From:**	
	Comments:	

CITATION
Ogawa, K., et al., "Phase Defect Inspection by Differential Interference", Lasertec Corporation (12 pages).
Kang, D., et al., "Effects of Mask Bias on the Mask Error Enhancement Factor (MEEF) of Contact Holes" (11 pages).
Socha, R., et al., "Printability of Phase-Shift Defects Using a Perturbational Model", Univ. of California Berkeley, Sematech (11 pages).
Erdmann, A., "Topography Effects and Wave Aberrations in Advanced PSM-Technology", Fraunhofer Institute of Integrated Circuits (11 pages).
Fiekowsky, P., "The End of Thresholds: Subwavelength Optical Linewidth Measurement Using the Flux-Area Technique", Automated Visual Inspection (6 pages).
Neureuther, A., "Modeling Phase Shifting Masks", SPIE, 10th Annual Symposium On Microlithography, Vol. 1496, pp. 80-85 (1990).
Watanabe, H., et al., "Detection and Printability of Shifter Defects in Phase-Shifting Masks", Japanese Journal of Applied Physics, Vol. 30, No. 11B, pp. 3016-3020, November 1991.
Hosono, K., et al., "A Novel Architecture for High Speed Dual Image Generation of Pattern Data for Phase Shifting Reticle Inspection", SPIE - Integrated Circuit Metrology, Inspection, and Process Control VI, Vol. 1673, pp. 229-235 (1993).
Obtsuka, H., et al., "Evaluation of Repair Phase and Size Tolerance for a Phase-Shift Mask", J. Vac. Sci. Technol. B, Vol. 11, No. 6, pp. 2665-2668, November/December 1993.
Reynolds, J., "Elusive Mask Defects: Reflectivity Variations", Solid State Technology, pp. 75-76, March 1995.
Kusunose, H., et al., "Direct Phase-Shift Measurement with Transmitted Deep-UV Illumination", SPIE, Vol. 2793, pp. 251-260 (1996).
Brunner, T., "Impact of Lens Aberrations on Optical Lithography", IBM J. Res. Develop., Vol. 41, No. 1/2, pp. 57-67, January/March 1997.
Tsujimoto, E., et al., "Hierarchical Mask Data Design System (PROPHET) for Aerial Image Simulation, Automatic Phase-Shifter Placement, and Subpeak Overlap Checking", SPIE, Vol. 3096, pp. 163-172 (1997).
Schoenmaker, W., et al., "Theory and Implementation of a New Interpolation Method Based on Random Sampling", IMEC Technology Paper, pp. 1-35, 31 January 1997.

FRED FERRIS
AU. 2123
TEL: 305-9670

Evaluation of repair phase and size tolerance for a phase-shift mask

Hiroshi Ohtsuka, Kazuyuki Kuwahara, and Toshio Onodera
V-LSI R&D Center, Oki Electric Company, Ltd., 550-1, Higashiasakawa-cho, Hachiojishi, Tokyo 193, Japan

(Received 5 June 1993; accepted 14 July 1993)

The conjugate twin-shifter method for alternating phase-shift method provides the flexibility for mask shifter layout, and is applied for both isolated and periodic shifter arrays in conventional *i*-line positive resist processes. A new mask structure simplifies shifter pattern delineation and reduces the effects of phase defects. The detail of intermediate phase interference has been analyzed by applying the two-dimensional shifter array as the phase defect. The results of this analysis provides the optimum repair element array for the new repair method of phase defects. Then the effectiveness of this simple repair method is examined in the *i*-line process by using the test arrays that delineated in the XeF_2 assisted focused ion beam process.

I. INTRODUCTION

The phase-shift method (PSM) provides the high resolution without loss of depth of focus (DOF), but the phase defects in shifter arrays degrade both resolution and DOF.[1,2] Printing of artifacts and degradation of effective DOF for critical dimension (CD) control are caused by changes in optical intensity and defocus characteristics. Phase defects are generally more serious than defect in opaque films, and are more difficult to repair.[3,4]

A simple repair method has been developed for alternating PSM. This technique is based on the analysis of randomly shaped phase defects that shows that symmetric arrays of small defects do not produce the defectlike artifacts. This result is applied for substituting new symmetry through the simple process steps.[5] This technique is utilized on the new film structure of conjugate twin-shifter mask and simple repair process that used XeF_2 assisted focused ion beam (FIB) milling process for generating repair element arrays. The effectiveness of this method is demonstrated in *i*-line positive resist process.

II. STRUCTURE OF CONJUGATE TWIN-SHIFTER MASK

Conjugate twin-shifter masks use three optical phases P0=0, P1=$-\pi/2$, and P2=$\pi/2$. This structure provides π relative phase difference between adjacent windows for alternating shifter arrays while simultaneously limiting phase transition of $\pi/2$ at the edge of shifter pattern arrays. The relative phase difference between the P1 and P2 shifters enhances image contrast. The $\pi/2$ relative phase difference between (P1–P0) and (P2–P0) shifters reduce the contrast of shifter edges and eliminates the printing of shifter edges. These shifter combinations improve the flexibility of phase shifter layout for use with complicated circuit patterns.

In the mask fabrication process, the two different $\pi/2$ film structures are generated by combining layer of spin on glass (SOG) and sputtered SiO_2. These films are deposited over the Cr opaque patterns on e-beam conductive film ($Ta_pO_r/Sn_xSb_yO_z$), shown in Fig. 1.

The bottom $\pi/2$ stacked layers are deposited on the first sputtered SiO_2 that consisted of SOG and second sputtered SiO_2 film for a multilayer cumulative shift of $\pi/2$. The top $\pi/2$ layer is formed over the first $\pi/2$ layer with a single SOG film. In the completed mask structure, the unshifted substrate material serves as the zero phase of P1 elements while the adjacent P2 shifter windows are formed by the cumulative effects of the first and second $\pi/2$ layers.

The two step etching improves phase accuracy by limiting phase errors to a maximum of $\pi/2$. SiO_2 etch barriers prevent defects from affecting more than $\pi/2$ layer at a time. The lower SiO_2 barrier protects the optically absorbing e-beam conductive film of for transmission uniformity.

The thickness of the first SOG film is made 3000 Å thicker than original film to supplement program defects and repair elements in the alternating shifter arrays. This modification provides adequate film thickness for FIB milling process to eliminate local intensity variations caused by removing the e-beam conductive film.

III. PHASE DEFECT MODEL

Phase angles of defects produced in the mask fabrication process are usually arbitrary, and these intermediate phase (not multiple of πN, N:integer) cause change in defocus characteristics even though they might not cause printed defects. In practice, arbitrary shifter width are used for circuit patterns, which makes analysis complex because of two-dimensional (2D) geometric effects.

The influence of phase defects on isolated patterns is analyzed by using the 2D defect model shown in Fig. 2. To simplify analysis, the horizontal widths of defects are assumed to equal to the window widths. An isolated opaque line between the P1 and P2 shifters abuts an edge of phase defect P_d, and the opposite edge of defective area P_d is assumed to be far enough away to neglect its optical interference with opaque line. This model will show the influence of repair element of arbitrary width, length L_d and phase P_d, located within an alternating shifter window. The location within a large clear area of P1 increases flexibility for analyzing repair tolerances because there is adequate space for optimized repair elements. The influence of this defect is analyzed for different value of length L_d

 0734-211X/93/11(6)/2665/4/$1.00

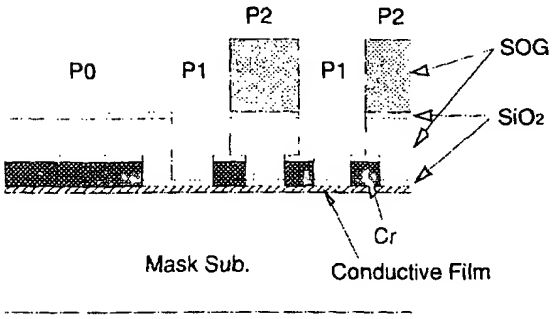

FIG. 1. New structure of conjugate twin-shifter phase shift mask with stacked transparent layers on opaque pattern used to delineate three different phase of P0, P1, and P2 in different process steps.

and different focal positions. The results provide the optimum conditions for shifter element repairs.

IV. INFLUENCE OF DEFECT SIZE

Defects with intermediate angles (unequal to πN, N:integer) cause two major types of problems; (1) reduction of intensity and (2) asymmetric focal effects caused by defocusing in opposite directions. Loss of intensity is worst when the phase errors is an integer multiple of π, and is less serious for values larger or smaller than an integer multiple.

Negative phase errors are used in this analysis that because the void-type defects result in shorter optical paths. Arbitrary phase angles for both residue- and void-type result in the same phase angles after being repaired using FIB milling process. A maximum defect phase of $-\pi/2$ that corresponds to missing half of nondefective shifter thickness is used, because of the error-limiting nature of the mask structure and repair process. Simulation results are shown in Figs. 3 and 4 for a defect of length L_d and intermediate phase.

Optical intensity at the edge of an opaque pattern determine the ability to control the CD. The cross-sectional intensity profile of an opaque line defocused positive 1.0 μm ($F=1.0\ \mu$m), shown in Fig. 3 (line A–B in Fig. 2), is

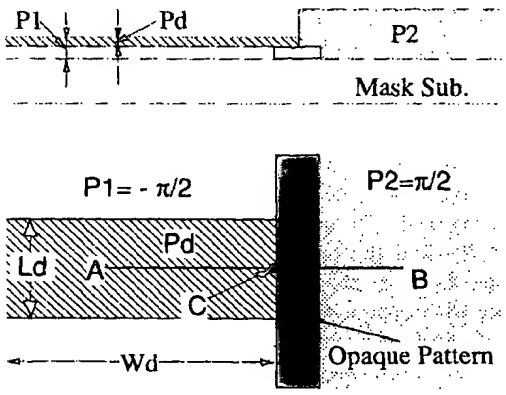

FIG. 2. 2D phase defect model for isolated feature. The length L_d phase defect of arbitrary phase abuts 0.3 μm opaque pattern in P1$=-\pi/2$ phase shifter. Optical conditions are i-line, NA=0.5 and $\sigma=0.5$.

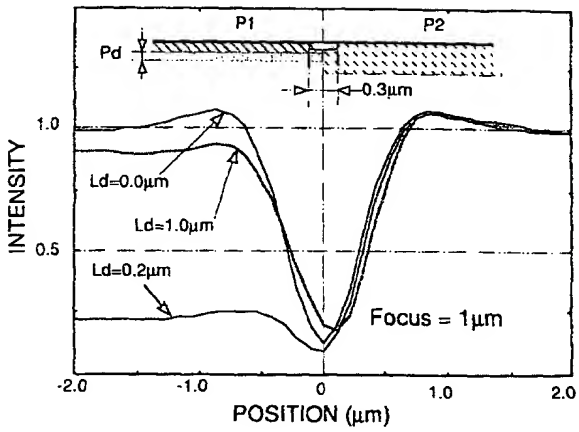

FIG. 3. Intensity of cross section A–B, in Fig. 2, is changed by different defect length of L_d for minus $\pi/2$ Phase (void-type defect) at 1.0 μm defocus position. Reduced intensity of $L_d=0.2\ \mu$m is restored by increased L_d of 1.0 μm.

altered by the presence of void-type phase defect of $P_d=-\pi/2$. Intensity of the nondefective side P2 is affected slightly, and is negligibly influenced by changes in defect size. On the P1 side where defect is located, the small defect $L_d=0.2\ \mu$m) seriously reduces the optical intensity while the large defect ($L_d=1.0\ \mu$m) provides intensity similar to the nondefective side. Another effect of intermediate phase is observed at the vertex of minimum intensity. The location of vertex, originally placed at the center of opaque line, is displaced toward the nondefective side with increased intensity. Direction of displacement and change of intensity are reversed by changing defocus direction to opposite. Asymmetric intensity changes, caused by defocusing in opposite directions, is another important factor. The magnitude of this effect also changes with the size of the phase error, and is maximized for errors near $\pi/2$. Further increases in defect phase reduces this effect and become zero for errors that are integer multiple of π.

The change of intensity on point C of opaque pattern edge (Fig. 2) is shown in Fig. 4 for different focus positions and defect phases. In negative 1.0 μm defocusing, negative defect phase of $-\pi/2$ small size defects slightly reduce the intensity of nondefective pattern edges ($L_d=0$), but intensity remains high above the best focus position regardless of defect length L_d. The serious influence of this defect type is caused in positive defocus direction that largely decrease the intensity while increasing in negative defocusing. Positive defocusing of 1.0 μm reduces intensity almost to zero for $L_d=0.3\ \mu$m; but intensity is increased larger values of L_d, reaching the original best focus value when $L_d=1.0\ \mu$m. The difference of these intensity with different defocusing is reduced by longer L_d and minimized around length of $L_d=1.0\ \mu$m.

This defocus asymmetry seriously degrades effective DOF required for CD control. Small phase errors reduce the seriousness of this problem, and phase errors of $\pi/4$ cause small difference of intensity. The geometric effect is minimized by using the optimized size of 1.0 μm for re-

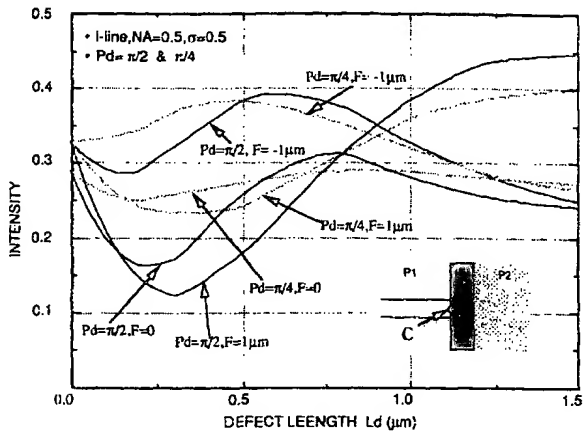

FIG. 4. Change of pattern edge intensity by defect length for different focus position and defect phases. Positive defocusing seriously reduces minimum intensity, but is increased to original intensity by larger values of L_d around 1.0 μm defect length. Defocus intensity difference of $-\pi/2$ (asymmetric defocus intensity change) is largely reduced by smaller defect phase of $-\pi/4$.

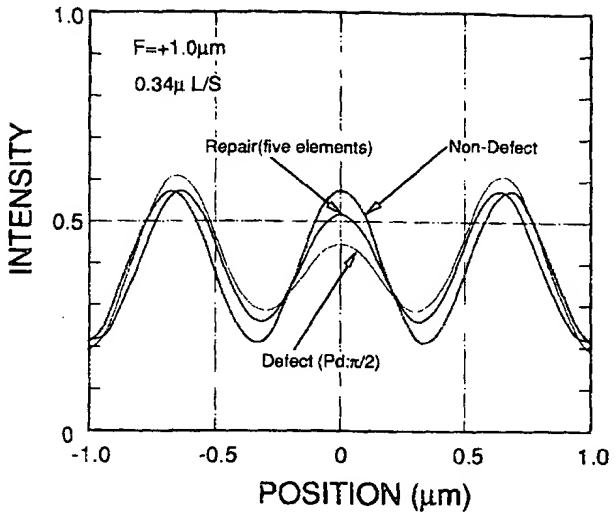

FIG. 6. Optical intensity profile of repaired area (cross section of A–B in Fig. 5). Reduced intensity of $-\pi/2$ phase defective window is restored more than 90% of original intensity by $-\pi/2$ phase step repair elements.

pairs, which effectively restores the intensity for phase transition of $\pi/4$ or less.

V. OPTIMIZED REPAIR MODEL

The problems of phase defect in alternating shifter arrays are caused by the locally produced asymmetric layout by undesired phase. This defective area degrades the DOF by causing the degradation of symmetric defocus characteristics, but the magnitude of this influence depends upon the phase and size. The new repair method operates by introducing a symmetric array of artificial "defects" as repair elements that are similar in phase and shape to the original flaw. This element array substitutes a new symmetry to reduce the phase errors in place of the symmetry that was destroyed by the defect. The advantage of this method is simplified repair process requiring only FIB milling for both residue- and void-type defects.

In the repair model, the defective portion of random phase surface is assumed to be repaired in milling process for the planarized surface of 1.0 μm length with $-\pi/2$ phase difference from original nondefective film. Repair elements can be delineated for arbitrary defect phases through use of the stacked film structure which functions as the end detection layer. This repair length is sufficient for minimizing the influence of $\pi/2$ phase error, but does not totally eliminate the influence of defects.

Effect of these phase errors are adequately reduced by introducing the allowable phase steps in arrangement of both repair elements in horizontal and vertical direction. The symmetric shifter layout with smaller phase step is delineated in adjacent windows because small phase defects often do not print when they are not sufficiently large to alter image intensity. The influence of $\pi/2$ phase error is

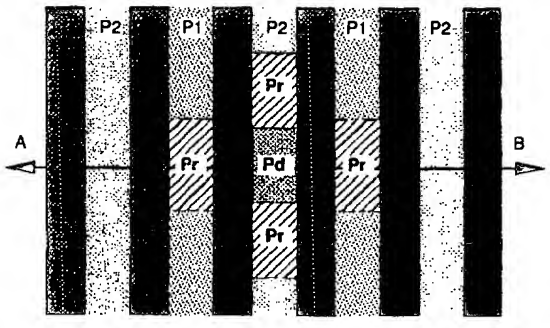

FIG. 5. Repair element arrays for $\pi/2$ phase defect in alternating shifter array. CD of each element include repaired defect (center of element array) are 1.0 μm. Number of repair elements is minimized by introducing the $\pi/4$ phase step as tolerance of phase error in both horizontal and vertical direction.

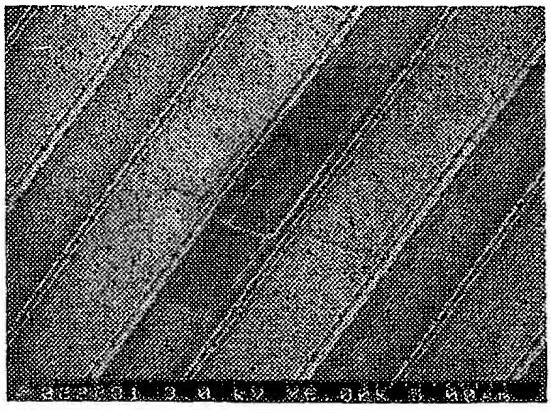

FIG. 7. Program repair arrays of test mask that delineated by XeF_2 assisted FIB system. Milling depths are ~1000 and 2000 Å for $-\pi/4$ and $-\pi/2$ elements. Milling process is completed with less Ga stained layer.

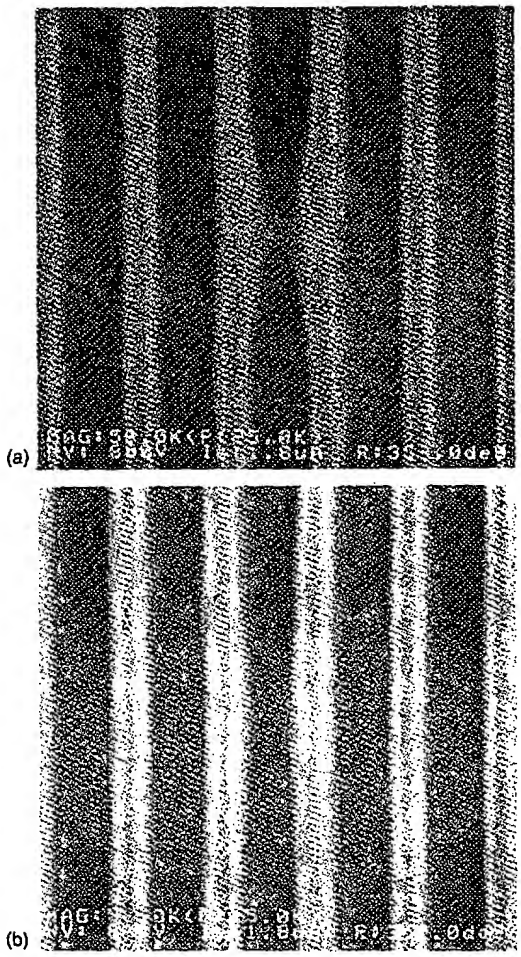

FIG. 8. Scanning electron microscope picture of patterning results of repaired $\pi/2$ phase defect by using repaired defect in Fig. 6. Center of phase defect is restored, but $-\pi/4$ phase transition in defective window is slightly increases the CD at the edge of repair element. (a) Before repair and (b) after repair.

reduced by introducing this phase step. Results of defect analysis show that phase errors of $\pi/4$ adequately reduce the influence of this effect. Additional $\pi/4$ elements are delineated in areas adjacent to the $\pi/2$ defect, causing the maximum relative errors to be $\pi/4$ in any one location. This array of $\pi/4$ phase step is adequate to restore the degraded defocus characteristics.

An optimized repair array for $\pi/2$ defects must contain at least five elements (Fig. 5); the $\pi/2$ defect repair element and four $\pi/4$ phase elements located in the windows adjacent to the defect. This five-element array of 1.0 μm length effectively restores the seriously reduced intensity of $\pi/2$ defect, shown in Fig. 6, in positive defocusing ($F=1.0$ μm) by more than 90% of nondefective window.

VI. EXPERIMENTAL RESULTS

The effectiveness of this method has been evaluated by using the programmed repair element, shown in Fig. 7, delineated by XeF_2 assisted FIB milling (micrion: 8000). The milling depth for each elements was determined by premilling test because the sputtered SiO_2 film end-point detection procedures were not utilized. A milling rate of 2 μm^3/min was sufficient for throughput, and repeatability of 10% was sufficient for the required phase accuracy. The edge of each element were slightly overlapped with the adjacent windows to eliminate the intensity reductions caused by registration errors. Patterning results in positive resist process (PFI-26,12 000 Å) by *i*-line (NA=0.5, $\sigma=0.5$) stepper are shown in Fig. 8. The $-\pi/2$ defective window is successfully separated with 0.6 μm defocing.

VII. CONCLUSIONS

Phase defects in alternating PSMs are repaired simply by using a new mask structure that limits maximum phase defects to $\pi/2$ or less in the mask fabrication process. In this simple repair method, the phase error of $\pi/2$ is divided into half with optimized geometric size. This smaller phase transition of $\pi/4$ adequately reduces the influence of defective areas in pattern delineation.

Size of repair elements is important in determining repair tolerance. Element size of longer than 1.0 μm are optimum, and defects smaller than 1.0 μm should be expanded to this length. The repaired phase step of $\pi/4$ is the tolerable phase error that restores 90% of original intensity. This phase step minimize the number of repair elements by five elements that arrayed in adjacent location of $\pi/2$ repair elements. The effectiveness of this method has been enhanced by the end-point detector material of sputter SiO_2 films in the shifter layers for use in the FIB milling process.

[1]M. D. Levenson, N. S. Viswanathan, and R. A. Simpson, IEEE Trans. Electron Devices ED-29 (1982).
[2]M. D. Prouty and A. D. Neureuther, Proc. SPIE 470 (1984).
[3]S. Okazaki, N. Hasegawa, and A. Imai, IEDM Tech. Dig. 1991, 55.
[4]H. Watanabe, Y. Todokoro, and M. Inoue, Jpn. J. Appl. Phys. 30, 3016 (1991).
[5]H. Ohtsuka, K. Kuwahara, T. Onodera, and T. Taguchi, Jpn. J. Appl. Phys. 31, 4143 (1992).

This Page is Inserted by IFW Indexing and Scanning Operations and is not part of the Official Record

BEST AVAILABLE IMAGES

Defective images within this document are accurate representations of the original documents submitted by the applicant.

Defects in the images include but are not limited to the items checked:

- ☐ BLACK BORDERS
- ☐ IMAGE CUT OFF AT TOP, BOTTOM OR SIDES
- ☑ FADED TEXT OR DRAWING
- ☐ BLURRED OR ILLEGIBLE TEXT OR DRAWING
- ☐ SKEWED/SLANTED IMAGES
- ☐ COLOR OR BLACK AND WHITE PHOTOGRAPHS
- ☐ GRAY SCALE DOCUMENTS
- ☐ LINES OR MARKS ON ORIGINAL DOCUMENT
- ☐ REFERENCE(S) OR EXHIBIT(S) SUBMITTED ARE POOR QUALITY
- ☐ OTHER: _____

IMAGES ARE BEST AVAILABLE COPY.
As rescanning these documents will not correct the image problems checked, please do not report these problems to the IFW Image Problem Mailbox.